Design and characterization of flavoenzyme models in the course of chemical evolution of four-α-helix bundle polypeptides

Kin-ya Tomizaki,[a] Yoshiro Tsunekawa,[a] Hideo Akisada,[b] Hisakazu Mihara[c] and Norikazu Nishino *[a]

[a] *Department of Applied Chemistry, Faculty of Engineering, Kyushu Institute of Technology, Tobata, Kitakyushu 804-8550, Japan*
[b] *Department of Environmental Chemistry, Faculty of Engineering, Kyushu Kyoritsu University, Yahata-nishi, Kitakyushu 807-8585, Japan*
[c] *Department of Bioengineering, Faculty of Bioscience and Biotechnology, Tokyo Institute of Technology, Nagatsuta, Yokohama 226-8501, Japan*

Received (in Cambridge, UK) 24th September 1999, Accepted 21st January 2000

The chemical evolution of four-α-helix bundle polypeptides to a flavoenzyme model was attempted by designing single-chain 53-peptides, which comprise flavin derivatives at three different positions. A pair of flavin derivatives were also introduced opposite to each other on the separate α-helix segments in the hydrophobic core. The four-α-helix bundle structure and the flavin moieties around the hydrophobic core were characterized by circular dichroism and fluorescence measurements, respectively. The flavoenzyme models were then examined for catalytic oxidation reaction of various *N*-alkyl-1,4-dihydronicotinamides (alkyl-NAHs) in aqueous solution. Since the hydrophobic core seemed to be too tightly aggregated for a catalytic group, a series of alkanesulfonates was tested to enlarge it by forming mixed micelles. The expanded hydrophobic core may more easily accommodate a hydrophobic substrate. Alkyl chains longer than dodecyl enhanced the oxidation of benzyl-NAH by a flavoenzyme model by about 6-fold. A series of alkyl-NAHs (*n*-butyl-, *n*-hexyl-, *n*-octyl-, *n*-decyl-, and *n*-dodecyl-NAHs) were also used as substrates in the oxidative reaction by flavoenzyme models to differentiate the positions of the flavin derivative with respect to the hydrophobic core according to their catalytic activities. The oxidation rate constants (k_{cat}/K_M) showed significant alkyl-chain-length dependence. The flavoenzyme models accommodated *n*-decyl- and *n*-dodecyl-NAHs favorably with K_M values in the (1.5–5.0) × 10^{-5} mol dm^{-3} range. These results suggest that the hydrophobic core in the bundle structure is useful to position the catalytic groups and has the advantage of accommodating hydrophobic substrates. Thus, there is the possibility to utilize the hydrophobic core of the polypeptide structure to evolve the artificial proteins chemically by *de novo* design towards artificial enzymes.

The four-α-helix bundle polypeptides have been attractive models of natural proteins, such as myohemerythrin and cytochrome *b*, from the beginning of the *de novo* design of artificial proteins.[1] In the last 10 years, several research groups demonstrated improvements in stability and new designs of protein-like features.[2–17] These efforts involve the so-called TASP (template assembled synthetic protein) strategy[5,6] and characterization by NMR[7,8] and other spectroscopic measurements.[9–11] Mutter and co-workers proposed a conceptually different approach in *de novo* design of protein (TASP concept) in order to bypass the protein folding problem.[5] The chemoselective ligation of unprotected peptide segments to the template molecules using thioester linkages was subsequently proposed as a route to the chemical synthesis of protein analogs of native topology.[6] Such progress in design and synthesis of large polypeptide molecules with four-α-helix bundle structure affords variety in further chemical evolution.

DeGrado and co-workers characterized dimerized four-α-helix bundle peptides and a single-chain four-α-helix bundle peptide by ^{1}H NMR measurements.[7,8] Below room temperature the NMR spectrum is reminiscent of a folded, tightly packed protein, while above room temperature it resembles what is typically observed for molten globules such as guinea pig α-lactalbumin.[12] Therefore, it is more likely that most of the four-α-helix bundle peptides designed *de novo* are in molten globule state.[2] Such molten globules may be also understood as a mixture of different packings of segments, because protein-like packing cannot be defined yet.

To characterize the four-α-helix bundle structure by other spectrophotometric measurements, Handel *et al*. incorporated a tryptophan residue, which is a dynamic fluorogenic amino acid, in the interior of a four-α-helix bundle peptide.[9] ANS (1-anilino-8-naphthalenesulfonate), which binds to apolar regions of molten globule proteins reflecting a mobile hydrophobic interior, was also employed in the characterization of synthetic four-α-helix bundle peptide.[8] We employed the tryptophan–dansyl group energy transfer system and excimer formation of pyrenylalanines to probe the α-helix bundle formation.[10,11] These environment sensitive fluorogenic groups were useful to characterize the designed single-chain four-α-helix bundle 53-peptides in molten globule state. In addition, we attempted to characterize the hydrophobic core in the bundle structure for the future chemical evolution of novel functions.

From the early stage of the development of artificial proteins by *de novo* design, functionalization has variously been considered. Sasaki and Kaiser demonstrated aniline hydroxylase activity on their helichrome.[13] Åkerfeldt *et al*. reported proton channel activity on their tetraphilin.[14] Both helichrome and tetraphilin consisting of four α-helices were built on porphyrin templates. We designed and synthesized an artificial membrane-spanning four-α-helix bundle protein, which had a flavin functionality at the cysteine side chain in one of the α-helix segments on a manganese porphyrin template.[15] In this membrane-spanning electron transfer system, the flavin moiety played the role of a mediator between dihydronicotinamide (electron donor) and manganese porphyrin (electron acceptor).

DOI: 10.1039/a907730h

This journal is © The Royal Society of Chemistry 2000

(a)

a[1] PELLKAXAELLK[13]-
a[14]PELLKALAELLK[26]-
a[27]PELLKXXXELLK[39]-
a[40]PELLKALAELLKG[53]

53-Peptide	Substitution			
	X[8]	X[33]	X[34]	X[35]
1	L	C(Fl)	L	A
2	L	A	C(Fl)	A
3	L	A	L	C(Fl)
4	C(Fl)	A	C(Fl)	A

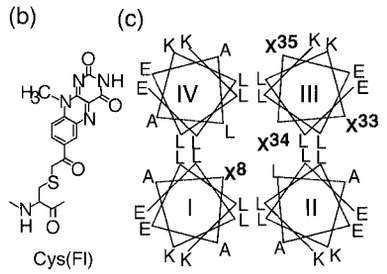

Fig. 1 Design of four-α-helix bundle polypeptides containing isoalloxazine rings: (a) amino acid sequences of four different 53-peptides, (b) structure of a isoalloxazine-linked cysteine, and (c) top view of the four-α-helix bundle structure. A = Ala, a = D-Ala, C = Cys, E = Glu, G = Gly, K = Lys, L = Leu, P = Pro.

The heme (iron–porphyrin complex)-assisted four-α-helix bundle structures with bis-histidine coordination to the iron were designed as models of cytochrome b_5 and cytochrome bc_1 and characterized by UV/vis and EPR spectroscopic measurements.[16] Rau and Haehnel also synthesized a cytochrome *b* model as a TASP, which binds two heme groups in four antiparallel helices on a cyclic decapeptide template.[17]

As an early example, decarboxylation of oxaloacetate was accelerated by aggregated amphiphilic and α-helical 14-peptides to form bundle-like structures, *i.e.*, oxaldie 1 and oxaldie 2.[18] Recently, Broo *et al.* reported the hydrolytic activity of a dimerized two-α-helix peptide toward *p*-nitrophenyl esters with rate enhancements, which were attributed to the cooperativity of unprotonated and protonated histidine residues in α-helix segments on the helix–loop–helix dimer.[19,20] Furthermore, the chiral recognition on hydrolysis of D- and L-norleucine *p*-nitrophenyl esters and specificity on hydrolysis of *p*-nitrophenyl alkanoates ($n = 1$, 2, 3, or 4) were demonstrated with the four-α-helix polypeptides dimerized with helix–loop–helix peptides.[21] The same group also reported site-selective glycosylation of a dimerized four-α-helix bundle peptide.[22] In the initial step the unprotonated form of the histidine side chain attacked the active ester of *p*-nitrophenyl 3-(1-thio-β-D-galactopyranosyl)propionate to form an acyl intermediate. In the second step the acyl group was transferred to the amine of the flanking lysine residue in a fast intramolecular reaction. The site-selective incorporation of the pyridoxal phosphate cofactor was also demonstrated.[23] The pyridoxal phosphate cofactor reacted with the side chain of the lysine residue flanking arginine to form an aldimine linkage. In their design, generally, the special amino acids histidine, lysine, and arginine were incorporated in the α-helix segments at the vicinity of the loop unit to place them closer to each other. When this helix–loop–helix peptide dimerizes to form four-α-helix bundle structure these hydrophilic amino acids may take positions at the surface of the bundle structure rather than in its hydrophobic core.

As summarized above, a new development is obviously aimed at the chemical evolution of four-α-helix bundle structure to the artificial enzymes. The most important aspect at present in *de novo* design is the positioning of catalytic functions under designed conditions, even in the molten globule state.

Since flavin coenzymes are prosthetic groups in a number of redox proteins and catalyse electron transfer, activation of dioxygen, and various monooxygenations, their chemical investigation has been fairly useful in the development of new catalysts.[24–27] Previously, we introduced flavin derivatives into four-α-helix bundle structure and preliminarily reported the activity.[28] The 53-peptides linked with flavin derivatives showed rate enhancements on oxidation of 1-benzyl-1,4-dihydronicotinamide (benzyl-NAH) and 1-*n*-hexyl-1,4-dihydronicotinamide (*n*-hexyl-NAH) in the presence of $(1.5–2.0) \times 10^{-3}$ mol dm^{-3} sodium dodecyl sulfate (SDS) relative to those in buffer solution, indicating that SDS molecules inserted into the hydrophobic core of the tight bundle structure allowed the efficient interaction between flavin moieties and substrate in the expanded mixed micelles. In the present study, we attempted to investigate the positioning of the flavin derivative in more detail in a single-chain four-α-helix 53-peptide, and to find out the relationship between the hydrophobicity and the catalytic activities. The position of the flavin derivative was shifted by one amino acid residue forward or backward from the center of the α-helix segment facing the hydrophobic core of the four-α-helix bundle structure (Fig. 1). In order to elucidate the role of hydrophobicity, we applied a series of surfactants to the catalytic oxidation reaction of these enzyme models. We also designed various substrates by combining alkyl chain tails with different lengths to dihydronicotinamide to probe the binding mode of substrates.

Results and discussion

Design and synthesis

An 11-peptide in the 53-peptide was designed to form an amphiphilic α-helical structure.[10,11,28] Four α-helix segments were combined with turning units of D-Ala-Pro. Five leucines and two pairs of glutamic acid and lysine were placed at the separate faces of the amphiphilic α-helical structure. A cysteine residue was incorporated at the 33rd, 34th, or 35th position in the third α-helix segment in place of alanine-33, leucine-34, or alanine-35 residue for model **1**, **2**, or **3** (Fig. 1). The model **2** has its flavin moiety in the most hydrophobic core formed by nineteen leucine residues inside of the four-α-helix bundle structure. The other models, **1** and **3**, have their flavin moieties one amino acid distant from the center core. These flavin moieties are expected to lie on the boundary between the surface and the core of the bundle structure, respectively (Fig. 2). Two cysteine residues were incorporated at the 8th and 34th positions in the first and the third α-helix segments for **4**, respectively. In this case both flavin moieties are placed face to face in the core and expected to exhibit any positive interaction.

Synthesis of 53-peptides[11,29] and attachment of flavin derivatives to the thiol side chains of cysteine residues[30–35] have been carried out according to the literature. In the synthesis of 53-peptides the convergent method was employed.[11,29] For a single α-helix segment, two protected short peptides were prepared by solid phase synthesis on *p*-nitrobenzophenone oxime resin using Boc chemistry. They were condensed to give each α-helix segment yet protected as starting intermediates to be built in the 53-peptide stepwise by 1-(3-dimethylaminopropyl)-3-ethylcarbodiimide hydrochloride (EDC·HCl) and 1-hydroxybenzotriazole monohydrate (HOBt·H_2O) (EDC–HOBt method)[11b,36] in solution. The side chains of cysteine, glutamic acid, and lysine were protected with 4-methylbenzyl (MeBzl), cyclohexyl ester (OcHex), and 2-chlorobenzyloxycarbonyl (ClZ), respectively, and the α-carboxyl group of glycine was protected with benzyl ester (OBzl). All α-helix segments, Boc-D-Ala-Pro-Glu(OcHex)-Leu-Leu-Lys(ClZ)-Ala-X_1-Ala-Glu(OcHex)-Leu-Leu-Lys(ClZ)-OH, Boc-D-Ala-Pro-Glu(OcHex)-Leu-Leu-

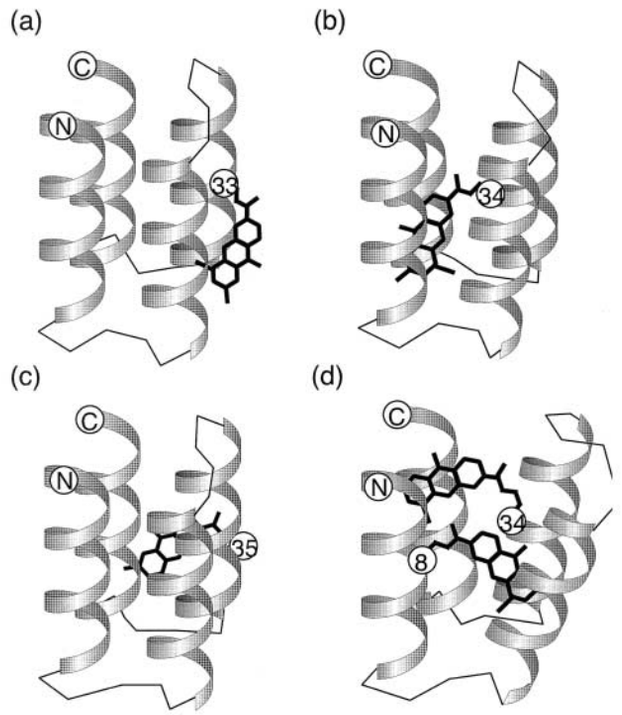

Fig. 2 Illustration of models **1** (a), **2** (b), **3** (c), and **4** (d). The isoalloxazine rings are shown at their corresponding positions from N-termini in amino acid sequences. Those in the hydrophobic core of **2** and **4** are expected to destabilize hydrophobic interaction among α-helix segments compared with those of **1** and **3**.

Lys(ClZ)-Ala-Leu-Ala-Glu(OcHex)-Leu-Leu-Lys(ClZ)-OH, Boc-D-Ala-Pro-Glu(OcHex)-Leu-Leu-Lys(ClZ)-X_2-X_3-X_4-Glu(OcHex)-Leu-Leu-Lys(ClZ)-OH, and Boc-D-Ala-Pro-Glu(OcHex)-Leu-Leu-Lys(ClZ)-Ala-Leu-Ala-Glu(OcHex)-Leu-Leu-Lys(ClZ)-Gly-OBzl, were characterized by HPLC and fast-atom-bombardment mass spectroscopy (FAB-MS).

The intermediates during the convergent elongation, protected 27-, 40-, and 53-peptides, were purified by gel filtration chromatography (Sephadex LH-60, DMF). The protecting groups were removed by anhydrous HF containing anisole and ethanedithiol for 90 min at 0 °C. 7α-Bromoacetyl-10-methylisoalloxazine (Br-AcFl) was attached to the cysteine side chain in crude 53-peptides under a nitrogen atmosphere and purified by gel filtration chromatography (Sephadex G-50, 10% acetic acid).[30a] The final purification was carried out on an HPLC column equipped with a gel filtration column (Superdex Peptide HR 10/30, 20% acetonitrile–0.1% TFA).

Solution molecular mass determination of 53-peptides linked with flavin derivatives was performed by gel filtration chromatography based on three marker proteins, cytochrome *c* (molecular weight, 12400), aprotinin (bovine lung, 6500), and insulin B-chain (bovine, 3496). The apparent molecular masses for all of the 53-peptides are summarized in Table 1. These values were somewhat larger than those obtained by matrix assisted laser desorption ionization time-of-flight mass spectrometry (MALDI TOF-MS). These differences of 2000–2500 masses most likely reflected the bulky flavin moieties in the peptides.[17,37] In amino acid analyses all amino acids except flavin-linked cysteine in 53-peptides were observed at theoretical values based on glycine. On the other hand, the Ellman reagent was inactive to the synthetic flavoenzyme models, indicating that the attachment of isoalloxazine rings to the thiol side chains of the cysteine residues in 53-peptides was quantitatively accomplished.

Circular dichroism (CD) studies of 53-peptides

All of the 53-peptides with four different sequences showed the typical α-helix circular dichroism pattern in aqueous solution:

Table 1 Molecular masses of model peptides **1**, **2**, **3** and **4**

Peptide	Theoretical	TOF-MS	Gel filtration chromatography[a]
1	5938.3	5942.6	8000 ± 600
2	5896.2	5900.5	7900 ± 500
3	5938.3	5942.7	8000 ± 600
4	6154.4	6158.3	8700 ± 500

[a] Performed on a Superdex Peptide HR 10/30 column eluted with 20% acetonitrile–0.1% TFA, flow rate 0.5 cm^3 min^{-1}.

Table 2 Circular dichroism data of 53-peptides

Peptide	$[\theta]_{222}$[a]/deg cm^2 $dmol^{-1}$	$C_{0.5}$ (GuHCl)[b]/ mol dm^{-3}
1	−21000	6.1
2	−19000	4.0
3	−21000	6.4
4	−17000	3.5

[a] Calculated molar ellipticity of the peptide at 222 nm in 0.1 mol dm^{-3} Tris–HCl buffer, pH 7.5 (containing 2% methanol) at 25 °C. [b] Midpoint of the transition to denaturation state calculated using a minimum ellipticity $[\theta]_{222} = -4000$ deg cm^2 $dmol^{-1}$.

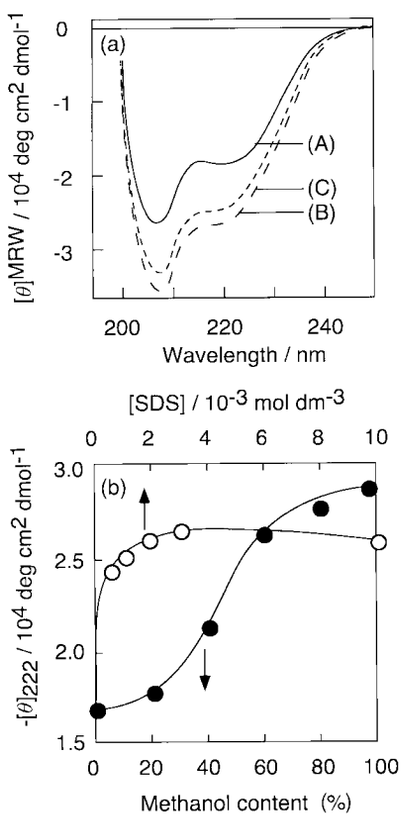

Fig. 3 (a) CD spectra of model **4** in 0.1 mol dm^{-3} Tris–HCl buffer, pH 7.5 (containing 2% methanol) (A), in methanol (B), and in the presence of 1.0×10^{-2} mol dm^{-3} SDS (C), at 25 °C. (b) Methanol (closed circles) and SDS (open circles) concentration dependence of ellipticity at 222 nm of **4**. [**4**] = 1.62×10^{-5} mol dm^{-3}.

a negative band corresponding to the amide n–π* transition in the vicinity of 220–222 nm, and a negative band near 208 nm as part of the exciton coupling of the amide π–π* transition. The ellipticities of **2** and **4** at 222 nm were $[\theta]_{222} = -19000$ and -17000 deg cm^2 $dmol^{-1}$, respectively (50–60% α-helicity). Since the loops connecting the helix segments should not be involved in the helix, the calculated α-helicity is estimated as about 70% (Fig. 3 and Table 2).[38] The other two peptides with one flavin on the surface of the bundle structure, **1** and **3**, showed slightly

higher α-helicity ($[\theta]_{222} = -21000$ deg cm^2 dmol^{-1}), probably due to the tighter packing and the higher hydrophobicity contributed by additional leucine-34 in the third segment. The 53-peptides **1**–**4** showed no significant changes in α-helicity at concentrations as low as 5.0×10^{-6} mol dm^{-3}, suggesting that they did not aggregate in aqueous solutions. When CD spectra of **4** were measured with increasing methanol content the α-helicity of **4** increased up to 77% (-28500 deg cm^2 dmol^{-1}). The methanol titration curve of ellipticity at 222 nm in the CD spectra of **4** showed a sigmoidal pattern with the midpoint at 45% methanol (Fig. 3). At higher methanol content the α-helical structure of **4** was stabilized by the enhancement of i, $i + 4$ hydrogen bonding rather than the hydrophobic interaction among the four α-helix segments.

No split CD induced by the two isoalloxazine rings in peptide **4** was observed probably due to their small transition moments in the visible region. In our previous work, 53-peptides containing a pair of L-1-pyrenylalanines (Pya) at the inner space of the four-α-helix bundle structure similar to **4** showed a split CD at 362 (positive peak) and 346 nm (negative peak) in less than 45% methanol.[11] This split CD disappeared with increasing methanol content. These results suggested that two pyrene rings were in close proximity with a right-handed twist according to the exciton chirality principle, even in the molten globule state of the bundle structure. Similarly, the two isoalloxazine rings of **4** are expected to be oriented in the hydrophobic core.

The thermodynamic stability of 53-peptides was examined by using guanidine hydrochloride (GuHCl) (Table 2). The addition of GuHCl to **1** and **3** linked with flavin derivatives at their outer positions resulted in a decrease in ellipticities at 222 nm in the CD spectra, consistent with the midpoint of denaturing to random coil structures ($C_{0.5}$(GuHCl)) at 6.1 mol dm^{-3} (**1**) and 6.4 mol dm^{-3} (**3**). In contrast, flavin derivatives placed in the hydrophobic cores of **2** and **4** resulted in $C_{0.5}$(GuHCl) values reduced to 4.0 and 3.5 mol dm^{-3} relative to those of **1** and **3**, respectively, indicating that the attachment of the isoalloxazine ring, a bulky tricyclic group, to the hydrophobic cores weakly destabilized their bundle structures.[34] In other words, the flavin derivatives of **1** and **3** are localized near the surface of the bundle structure.

Fluorescence properties of 53-peptides

The flavin derivatives incorporated into 53-peptides showed 1/5 reduced fluorescence at 510 nm (excited at 430 nm) per peptide-bound flavin derivative as compared with that of unbound AcFl. With increasing methanol content, the fluorescence intensity of peptide **4** increased gradually rather than characteristically depending on the methanol content toward a relative intensity of 2.1, accompanied by a blue-shift of λ_{max} from 511 to 504 nm (Fig. 4).[39] These results also suggest that **4** cannot stow two bulky isoalloxazine rings completely in its hydrophobic core at low methanol content, consequently their surroundings were partly similar to the bulk solvent.

The solvent accessibility of the flavin derivatives placed at the inner spaces in peptides **2** and **4** were compared to those of the chromophores at the surface in **1** and **3** by measuring the collisional quenching of the flavin fluorescence by iodide ions (Fig. 5 and Table 3).[34,40] The relative flavin fluorescence was plotted against the iodide concentration ([Q]). The data were fitted by the modified Stern–Volmer equation to obtain values for dynamic (K_{SV}) and static (v) quenching. The dynamic quenching constant, K_{SV}, for **2** was 8–9 times smaller than those for **1** and **3**. The K_{SV} value for **4** was also approximately 1.5 times smaller than those for **1** and **3** but 5.5 times greater than that for **2**. These differences in the magnitude of K_{SV} values for the peptides most likely suggest that the flavin moiety in **2** was significantly shielded from quencher in bulk solvent, relative to those at the surface in **1** and **3**. The peptide matrix of **4** could not shield completely two isoalloxazine rings from quencher,

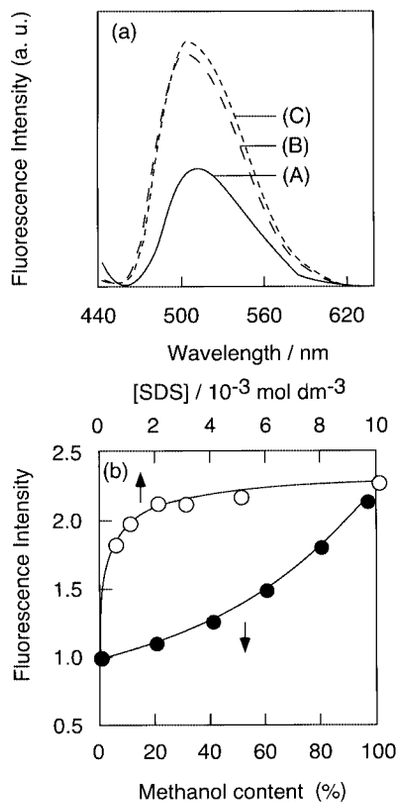

Fig. 4 (a) Fluorescence spectra of peptide **4** in 0.1 mol dm^{-3} Tris–HCl buffer, pH 7.5 (containing 2% methanol) (A), in methanol (B), and in the presence of 1.0×10^{-2} mol dm^{-3} SDS (C), excited at 430 nm at 25 °C. (b) Methanol (closed circles) and SDS (open circles) concentration dependence of fluorescence intensity at the vicinity of 510 nm. [**4**] = 2.0×10^{-6} mol dm^{-3}.

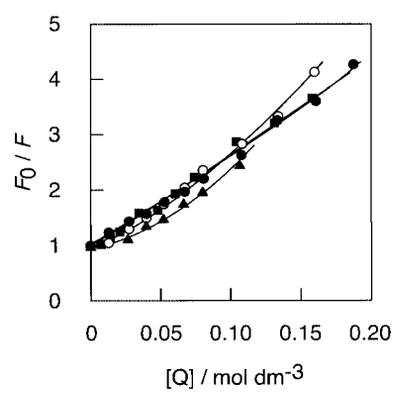

Fig. 5 Stern–Volmer plots of iodide quenching of fluorescence of the flavin derivative in peptides **1** (closed circles), **2** (closed triangles), **3** (closed squares), and **4** (open circles) in 0.1 mol dm^{-3} Tris–HCl buffer, pH 7.5 (containing 2% methanol) at 25 °C. The solid lines are the optimized fits of the data by the modified Stern–Volmer equation. [Peptide] = 5.0×10^{-6} mol dm^{-3}.

thus the bulk solvent is easily accessible to them in the bundle structure of **4**. The K_{SV} value for **1** was slightly smaller than that for **3**, indicating that the flavin moiety in **1** was placed nearer than that in **3**. On the other hand, the V values for 53-peptides exhibited the opposite behavior compared with their K_{SV} values, indicating that the movement of the iodide ions in the hydrophobic core may be suppressed. The magnitude of the K_{SV} values and the $C_{0.5}$(GuHCl) values for 53-peptides were in good agreement.

Effects of sodium dodecyl sulfate

As observed above, the bundle structure, even in the molten globule state, seemed to be so tightly aggregated to the flavin

Table 3 Fluorescence quenching parameters[a]

Peptide	K_{SV}/dm^3 mol^{-1}	V/dm^3 mol^{-1}
1	12.9	1.2
2	1.7	6.9
3	14.9	0.7
4	9.4	3.1

[a] Estimated from the Stern–Volmer plots of iodide quenching of flavin fluorescence fitted by the equation, $F_0/F = (1 + K_{SV}[Q])\exp([Q]V)$ in 0.1 mol dm^{-3} Tris–HCl buffer, pH 7.5 (containing 2% methanol) at 25 °C. [Peptide] = 5.0×10^{-6} mol dm^{-3}.

moiety that we tried to enlarge the hydrophobic core of many leucine side chains by adding surfactants. Since we previously observed that the Pya containing 53-peptide accommodated an acridine orange dye with longer alkyl chain than the dodecyl group with 1 : 1 stoichiometry, in the present study we tried to form a complex between **4** and SDS molecules.[41] At 2.0×10^{-3} mol dm^{-3} SDS in aqueous solution, the ellipticity at 222 nm of **4** interestingly increased 1.5 times greater than that in the absence of SDS although this SDS concentration is lower than that of the critical micelle concentration (CMC) (Fig. 3). The fluorescence intensity of **4** also increased 2.2 times greater than that of in the absence of SDS, accompanied by a blue-shift of λ_{max} from 511 to 507 nm (Fig. 4). **4** showed saturated ellipticity at 222 nm and saturated fluorescence intensity at above 3.0×10^{-3} mol dm^{-3} SDS. The SDS molecules were likely accommodated into the hydrophobic core of the bundle structure, consequently mixed micelles may be formed with **4** and SDS. Thus, we further attempted to utilize this inner space of the four-α-helix bundle structure with surfactant to capture the hydrophobic groups of substrates.

Oxidation of 1-benzyl-1,4-dihydronicotinamide (benzyl-NAH) in the presence of a series of sodium alkanesulfonates

The initial rate constants (v_0) of alkyl-NAH oxidation by flavoenzyme models were obtained by measuring the decrease in absorption intensity at 360 nm according to the literature.[28] The v_0 values were estimated from the less than 10% consumption of benzyl-NAH to minimize the influences of side reactions such as degradation of peptide and hydroxylation of the aromatic ring. The kinetic parameters (k_{cat}, K_M, and k_{cat}/K_M) were calculated from substrate concentration *vs.* v_0 plots fitted by the Michaelis–Menten equation, $v_0 = k_{cat}$ [peptide][S]/(K_M + [S]), where v_0 is the initial rate, [peptide] the total peptide concentration, and [S] the substrate concentration.

Preliminarily, we found that the addition of SDS enhanced the second-order-rate constant for oxidation of benzyl-NAH by peptide **4** by 2.5 times and that the maximum rate constant was given in the presence of 2.0×10^{-3} mol dm^{-3} SDS.[28] From these results, we assumed that the tight bundle structure was expanded by SDS and accommodates substrate into the hydrophobic core efficiently. Therefore, we focused attention on the relationship between the oxidation rate constants and the alkyl chain length of the surfactants. Fig. 6 shows the effects of sodium alkanesulfonates (*n*-hexane-, *n*-octane-, *n*-decane-, *n*-dodecane-, *n*-tetradecane-, and *n*-hexadecanesulfonate) on the oxidation of benzyl-NAH catalysed by **4** and AcFl as a reference compound. Without surfactants, **4** oxidized benzyl-NAH 3.5 times faster than AcFl, consequently the rate was accelerated only 1.75 times per flavin. **4** exhibited bell-shaped benzyl-NAH oxidation kinetics depending on the surfactant concentration. The hydrophobic core in the bundle structure recognized the hydrophobic group in benzyl-NAH. With longer alkanesulfonates, *e.g.* *n*-dodecane-, *n*-tetradecane-, and *n*-hexadecanesulfonates, **4** showed the maximum rate enhancement compared with the rates in the absence of surfactant (1.4×10^3 dm^3 mol^{-1} s^{-1}, 5.6 times greater than those of AcFl). All

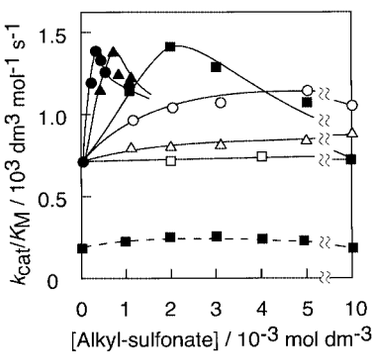

Fig. 6 Kinetic parameters (k_{cat}/K_M) for oxidation of benzyl-NAH catalysed by peptide **4** (solid line) and second-order-rate constants for AcFl (dashed line) depending on the concentrations and alkyl chain length of surfactants: *n*-Hexadecanesulfonate (closed circles), *n*-tetradecanesulfonate (closed triangles), *n*-dodecanesulfonate (closed squares), *n*-decanesulfonate (open circles), *n*-octanesulfonate (open triangles), and *n*-hexanesulfonate (open squares) in 0.1 mol dm^{-3} Tris–HCl buffer, pH 7.5 (containing 2% methanol) at 25 °C. The data were fitted by the Michaelis–Menten equation. [**4**] = [AcFl] = 8.4×10^{-7} mol dm^{-3}, [benzyl-NAH] = (0.5–2.2) × 10^{-4} mol dm^{-3}.

of the surfactant concentrations where the maximum rates were obtained were lower than their corresponding CMCs (1.05×10^{-3} mol dm^{-3}, *n*-hexadecane-; 2.5×10^{-3} mol dm^{-3}, *n*-tetradecane-; 1.0×10^{-2} mol dm^{-3}, *n*-dodecane-; 4.4×10^{-2} mol dm^{-3}, *n*-decane-; 0.155 mol dm^{-3}, *n*-octane-; 0.46 mol dm^{-3}, *n*-hexanesulfonates, respectively). No significant rate enhancements, in AcFl catalysed oxidation of benzyl-NAH, were observed in the presence of *n*-dodecanesulfonate. The large excess of these surfactants, however, inhibited the interaction between flavin moieties and the substrate, consequently the oxidation rate constants for catalysis by **4** were decreased. In the **4**–benzyl-NAH system the shorter alkanesulfonates showed very weak rate enhancements, 1.6-fold with *n*-decanesulfonate, 1.2-fold with *n*-octanesulfonate, and no effect with *n*-hexanesulfonate compared with that in the absence of surfactants. Upon addition of a surfactant with long enough alkyl group, the hydrophobic core made of leucine side chains may form a kind of mixed micelle in the bundle structure. Thus the molten globule inserted with surfactants is supposed to offer an extended reaction field, where the substrate is accessible and the product can leave as observed in an enzymatic reaction center.

Oxidation of a series of 1-*n*-alkyl-1,4-dihydronicotinamides

Since the flavoenzyme model **4** accommodated benzyl-NAH efficiently in the presence of *n*-dodecane-, *n*-tetradecane-, and *n*-hexadecanesulfonates as described above, we modified dihydronicotinamide with a series of *n*-alkyl groups to reinforce the hydrophobicity.[42] The nicotinamide was treated with five different *n*-alkyl iodides and the *N*-substituted nicotinamide iodides were then reduced by sodium dithionite to the corresponding *n*-alkyl-dihydronicotinamides (*n*-butyl-, *n*-hexyl-, *n*-octyl-, *n*-decyl-, and *n*-dodecyl-NAHs). All alkyl-NAHs were purified by silica gel chromatography and stored in methanol.

Kinetic parameters for the oxidation of five different alkyl-NAHs catalysed by flavoenzyme models (**1**–**4**) are summarized in Table 4 as a function of alkyl chain lengths. With longer alkyl chains, the K_M values for **1**, **2**, and **3** were significantly decreased. In the presence of *n*-butyl, *n*-hexyl-, and *n*-octyl-NAHs the peptide–substrate complex was unstable, resulting in large K_M values. In the presence of *n*-decyl- and *n*-dodecyl-NAHs, **1**, **2**, and **3** favorably accommodated the substrate, giving small K_M values. The K_M values of the *n*-hexyl-, *n*-octyl-, *n*-decyl-, and *n*-dodecyl-NAHs, especially *n*-octyl-NAH, for **4** were greater than those for **1**, **2**, and **3**. Fig. 7 shows the binding properties ($1/K_M$) between 53-peptides and the series of alkyl-NAHs as a function of the number of methylene groups. **1**, **2**,

Table 4 The kinetic parameters for the oxidation of 1-*n*-alkyl-1,4-dihydronicotinamides catalysed by flavoenzyme models[a]

	k_{cat}, K_M, k_{cat}/K_M				
Peptide	*n*-butyl-NAH[b]	*n*-hexyl-NAH[b]	*n*-octyl-NAH[b]	*n*-decyl-NAH[c]	*n*-dodecyl-NAH[d]
1	0.20, 300, 670	0.18, 150, 1200	0.18, 70, 2600	0.20, 30, 6500	0.20, 15, 13000
2	0.22, 350, 630	0.20, 150, 1300	0.19, 60, 3200	0.19, 25, 7600	0.21, 15, 14000
3	0.20, 300, 670	0.19, 150, 1300	0.16, 70, 2300	0.16, 30, 5300	0.18, 15, 12000
4	0.63, 300, 2100	0.65, 200, 3300	0.68, 150, 4500	0.72, 50, 14000	0.72, 20, 36000

[a] Calculated from the initial rates at 8–12 different substrate concentrations. [Peptide] = 8.4×10^{-7} mol dm^{-3} in 0.1 mol dm^{-3} Tris–HCl buffer, pH 7.5 (containing 12% methanol) at 25 °C. The units of k_{cat}, K_M, and k_{cat}/K_M are s^{-1}, 10^{-6} mol dm^{-3}, and dm^3 mol^{-1} s^{-1}, respectively. [b] (5–250) $\times 10^{-6}$ mol dm^{-3}. [c] (5–100) $\times 10^{-6}$ mol dm^{-3}. [d] (5–50) $\times 10^{-6}$ mol dm^{-3}.

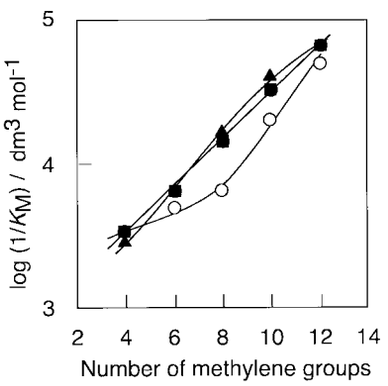

Fig. 7 Binding properties between peptides **1** (closed circles), **2** (closed triangles), **3** (closed squares), and **4** (open circles) and the series of alkyl-NAHs in 0.1 mol dm^{-3} Tris–HCl buffer, pH 7.5 containing 12% methanol at 25 °C as a function of the number of methylene groups of the substrates. The $1/K_M$ values were obtained from the data in Table 4.

and **3** exhibited a logarithmic increase rather than linear with the number of methylene groups in the alkyl chain of the substrates. The flavoenzyme model **4** did not recognize alkyl-NAHs with short alkyl chains, as well as the other three peptides, because a pair of flavin moieties in the hydrophobic core of **4** destabilized slightly the hydrophobic interaction among the α-helix segments compared with the other peptides having one flavin, as observed in GuHCl denaturation and flavin fluorescence quenching measurements. However, with longer alkyl chains of the substrates, the $1/K_M$ values for **4** gained steadily and reached those for **1**, **2**, and **3** for *n*-dodecyl-NaH. These facts are reasonable to understand in that the relaxed **4** with a pair of flavin moieties recognized the long alkyl chain of substrate by means of 'the induced fit mechanism'.

On the other hand, it was expected that the k_{cat} values for **4** would be less than twice those for **1**, **2**, and **3** due to the number of flavin moieties. However, the actual k_{cat} values for **1**, **2**, and **3** were very similar in the range 0.16–0.22 s^{-1}, and those for **4** were slightly increased from 0.63 to 0.72 s^{-1} with longer alkyl chains of dihydronicotinamide. The k_{cat} values for **4** were somewhat greater than twice those for **1**, **2**, and **3**. These differences in the magnitude of the k_{cat} values between **4** and the other peptides might reflect that **4** released more smoothly the oxidized product (now cationic with pyridinium moiety) than **1**, **2**, and **3** in the catalytic cycle. The k_{cat}/K_M values for flavoenzyme models significantly increased with longer alkyl chains of the substrate. The k_{cat}/K_M values for **2** were greater than those for **1** and **3** with longer alkyl chains. These differences in the magnitude of the k_{cat}/K_M values for flavoenzyme models with one flavin moiety strongly suggest that the flavin derivative placed at the center of the hydrophobic core is more favorable to oxidize longer alkyl-NAHs than those at the different positions on the surface of the bundle structure. Further, the k_{cat}/K_M values for **1** are slightly greater than those for **3**. These results are in good agreement to those observed in flavin fluorescence quenching measurements. The oxidation of the series of alkyl-NAHs except *n*-octyl-NAH catalysed by **4** showed rate enhancements relative to those for the other three peptides of more than twice. Thus, the differently increased oxidation rate constants for the four flavoenzyme models reflect the difference of the hydrophobic core formed in each model.

Kinetic parameters for several naturally occurring flavoenzymes and isoalloxazine-linked papain in the literatures are as follows: flavopapain (k_{cat}/s^{-1} 0.103; $K_M/10^{-6}$ mol dm^{-3}, 30; k_{cat}/K_M/dm^3 mol^{-1} s^{-1} 3500),[30] NADH specific FMN oxidoreductase (B. Harveyi) (15.5, 47.5, 3.3×10^5),[30,43] NADPH specific FMN oxidoreductase (B. Harveyi) (34.0, 40.0, 8.5×10^5),[30,43] and old yellow enzyme (Yeast) (0.71, 220, 3.2×10^3).[30,44] The K_M values, which we measured, for oxidation of *n*-octyl-, *n*-decyl-, and *n*-dodecyl-NAHs catalysed by flavoenzyme models are comparable to those found for NADH and NADPH oxidation catalysed by natural flavoenzymes. The turnover numbers (0.16–0.21 s^{-1}) of 53-peptides with one flavin moiety, **1**, **2**, and **3**, are smaller than those of NADH- and NADPH-specific FMN oxidoreductases by one order of magnitude. However, the turnover numbers of **4** are comparable to that of the old yellow enzyme.

Oxidation of *n*-decyl-NAH under denatured conditions with guanidine hydrochloride and methanol

In order to reveal the relationships between the catalytic activity and conformation of the synthetic flavoenzyme models, we oxidized *n*-decyl-NAH using 53-peptides linked with flavin derivatives under denatured conditions with GuHCl (Fig. 8(a)) and methanol (Fig. 8(b)). The profiles of the v_0 values observed with GuHCl showed bell-shaped kinetics. The maximum v_0 value for **2** at 1.5 mol dm^{-3} GuHCl was a factor of 2.0 greater than the initial rate without GuHCl. The maximum v_0 values for **1** and **3** at 1.5 mol dm^{-3} GuHCl were greater by a factor of 1.5. The maximum v_0 value for **4** at 0.4 mol dm^{-3} GuHCl was greater by a factor of 1.2 relative to the initial rate without GuHCl. With further addition of GuHCl to the solution the v_0 values for **1**, **2**, and **3** were decreased, and then the activities at 7.0 mol dm^{-3} GuHCl concentration remained about 15% of the maximum rates. It should be noted that the v_0 values for **4** decreased considerably at around 2.0 mol dm^{-3} GuHCl, and its activity was less than twice those for **1**, **2**, and **3** at 7.0 mol dm^{-3} GuHCl. The v_0 of unbound AcFl was not affected by the GuHCl concentration. At higher GuHCl concentrations, the α-helix in the bundle structure should be unwound to give a random coil, accordingly the hydrophobic core is demolished, resulting in the loss of efficient accommodation of substrates. The fact that the maximum v_0 value for **4** was observed at lower GuHCl concentration than those for **1**, **2**, and **3** suggests that the pair of flavin rings in **4** slightly destabilized the α-helical secondary structures compared with each flavin in **1**, **2**, and **3** as observed in measurements of the thermodynamic stability. Consequently, at a characteristic GuHCl concentration for each 53-peptide, the bundle structure may be relaxed moderately so as to be able to catch the substrate and to release the product smoothly. Furthermore, it is likely that the differences in the magnitude of the k_{cat} values for the oxidation of the series of alkyl-NAHs in aqueous solution

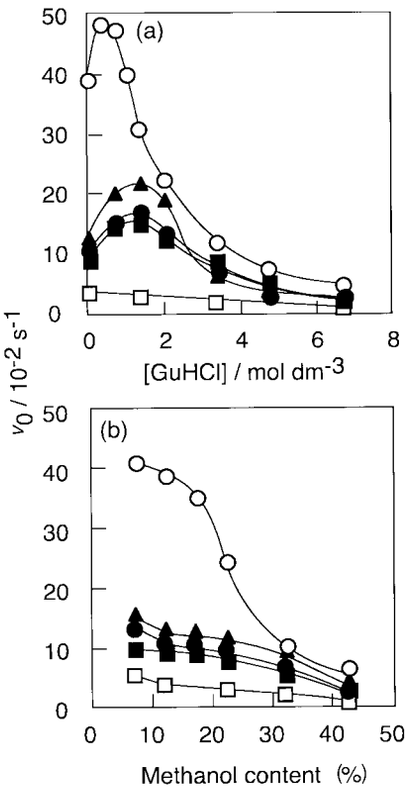

Fig. 8 The initial rates of *n*-decyl-NAH oxidation depending on (a) GuHCl concentration (0–7.0 mol dm^{-3}) and (b) the methanol content (7–42%) catalysed by peptides **1** (closed circles), **2** (closed triangles), **3** (closed squares), **4** (open circles), and AcFl (open squares) in 0.1 mol dm^{-3} Tris–HCl buffer, pH 7.5 (containing 12% methanol) at 25 °C. [Peptide] and [AcFl] = 8.4×10^{-7} mol dm^{-3}, and [*n*-decyl-NAH] = 5.0×10^{-5} mol dm^{-3}.

catalysed by 53-peptides indicate easy release of the oxidized substrates.

Methanol is well known to induce α-helix conformation and weaken the hydrophobic interaction of the bundle structure. We also examined the relationship between oxidation activity and methanol content (Fig. 8(b)). However, no maximum v_0 values were given at any methanol content, differently from those observed under the denaturation conditions with GuHCl. On adding methanol to the buffer solution, the oxidation activity catalysed by **1**, **2**, and **3** decreased toward 30% of those at 7% methanol content with the midpoint of 25% methanol content. **4** also showed a methanol content dependence of the oxidation of *n*-decyl-NAH. The v_0 values for **4** decreased remarkably with the midpoint at 22% methanol content, coincident to those for **1**, **2**, and **3**, consequently its activity was less than twice those for **1**, **2**, and **3** at 42% methanol content, because of the melting of the bundle structure. It may be difficult for a simple four-α-helix bundle polypeptide combined with only an α-helical secondary structure to show rate enhancement in a enzyme-like catalytic reaction. *De novo* designed polypeptides, as described here, tightly fold into a four-α-helix bundle structure with hydrophobic interaction in aqueous solution. Therefore, a characteristic denaturant concentration was required to achieve the favorable conformation of polypeptide for flavoenzyme-like alkyl-NAH oxidation.

Possibilities and limitations of artificial enzymes

Enzymes perform chemical reactions with high specificity and rate enhancement in aqueous media under mild conditions. Chemical investigation of the prosthetic groups, such as flavin coenzymes, have been fairly useful in the development of new catalysts. Kaiser and co-workers synthesized flavoenzyme models based on naturally occurring enzymes such as papain,[30] glyceraldehyde-3-phosphate dehydrogenase,[31] lysozyme,[32] and hemoglobin[33] modifying their cysteine side chains with Br-AcFl. Although most of these systems take advantage of substrate binding sites present in the starting enzymes, their specificities are limited by the structures of the native enzymes. Distefano and co-workers designed new catalysts based on the use of a protein cavity to accommodate a variety of substrates.[37] They introduced a pyridoxamine cofactor and 1,10-phenanthroline into a cysteine side chain in the cavity of adipocyte lipid binding protein (ALBP). Their phenanthroline binding-ALBP catalysed the enantioselective hydrolysis of several amino acid esters. However, these semisynthetic approaches also have some disadvantages, *i.e.* when a template enzyme has more than two cysteine residues or none, selective incorporation of the functional group into the enzyme is very difficult.

On the other hand, recently, a number of *de novo* designed polypeptides have emerged as one of the tools to construct the desired structures and to accomplish highly efficient and highly stereoselective chemical reactions.[1–23,28,34] We paid attention to the hydrophobic core formed in the four-α-helix bundle structure. In our single-chain 53-peptide system the hydrophobic core is made of twenty leucine side chains and is as non-polar as an organic solvent.[10,11] It is like a micro oil drop in water with a volume of less than 1000 $Å^3$ (10 Å high and less than 10 Å in diameter). The functional groups for enzymatic catalytic activity, such as the nucleophilic side chains of amino acids, are often buried in the hydrophobic inner space of the proteins. They usually lie at the bottom of the substrate binding sites with amazing mechanisms for catalytic reactions. Though the molten globule state does not give a strict conformation to the introduced functional groups, its hydrophobic core will offer supporting space for the reactivity. Thus, we introduced a flavin function into the hydrophobic core of four-α-helix bundle structure based on the literatures.[30–35] The flavoenzyme model **2** buries its flavin deep in the core. On the contrary, **1** and **3** tether their flavins apart from the hydrophobic core. They are not buried in the non-polar areas as probed by iodide ions. However, in the activities in oxidation of alkyl-NAHs, it was difficult to find a significant difference among the flavoenzyme models **1**, **2**, and **3**. These flavins are supposed to be working similarly judging from the k_{cat} and K_M values (Table 4). This fact may reflect the limitation of the molten globule state with catalytic function. Since a protein-like packing was not yet furnished, the functional groups behaved as if in solution of an organic solvent.

No flavoenzymes contain a pair of flavins in the same hydrophobic core like **4**. This peptide **4**, which binds a pair of flavins, showed different properties from the other three model 53-peptides in conformational stability and catalytic activity. It is less stable in conformation and less efficient than the other three in accommodating alkyl-NAHs with greater K_M values for all alkyl-NAHs (Table 4). However, it showed most efficient catalytic activity in the oxidation reaction. Under denaturing conditions, **4** responded more sensitively. Probably, two flavin moieties are too bulky to lie in the four-α-helix bundle structure of the 53-peptide. Though a specific interaction between a pair of flavins was not observed in the present study, a combination of flavin with other redox functional groups might construct a cooperative system in the polypeptide in future rational design.

We started this study with the hope that the designed polypeptides in the molten globule state may be functionalized and evolved chemically by tuning the positioning of the catalytic groups. The molten globule polypeptides may be primitive proteins, but have versatile peptide scaffolds which can be improved by incorporating specific electrostatic, hydrogen-bond, and van der Waals interactions. By such efforts, catalytic molten globules[45] could be evolved chemically toward native-like enzymes or artificial enzymes with novel functions.

Conclusion

We successfully incorporated flavin derivatives into single-chain 53-peptides and differentiated the arrangement of the catalyst in the four-α-helix bundle structure by CD measurements and iodide quenching experiments. We further demonstrated the use of the core of the four-α-helix bundle polypeptide as a hydrophobic substrate binding site for oxidation reaction by the flavin moiety. The resulting oxidation rate constants (k_{cat}/K_M) of alkyl-NAHs were significantly dependent on the alkyl chain length of the substrates, and the hydrophobic core consisting of 18–20 leucine side chains that could be controlled by long alkanesulfonates (alkyl group = *n*-dodecyl, *n*-tetradecyl, or *n*-hexadecyl) to allow the interaction of flavin moieties and benzyl-NAH. Furthermore, their chemical reactivities were also controlled by the use of a series of alkyl-NAHs (alkyl group = *n*-butyl, *n*-hexyl, *n*-octyl, *n*-decyl, or *n*-dodecyl) with hydrophobic interaction. *De novo* designed polypeptides will in future be engineered with more elaborately designed reactive sites and three-dimensional structure to recognize individual substrates specifically and to catalyse with large rate enhancements for chemical reactions.

Experimental

Chemicals and solvents

Amino acid derivatives and reagents for peptide syntheses were purchased from Watanabe Chemical Co. (Hiroshima, Japan) and Wako Pure Chemical Industries, Ltd. (Osaka, Japan). Analyses were followed by thin-layer chromatography (TLC) using silica gel (Kieselgel 60 F_{254}, Merck) and high performance liquid chromatography (HPLC) using a Hitachi HPLC system equipped with a Hitachi L-6300 Intelligent Pump, L-4200 UV-VIS Detector and D-2500 Chromato Integrator with a Wakopak C_4 column (4.6 × 150 mm; 120 Å, Wako Pure Chemical Industries, Ltd., Japan), eluted with linear 55–100% acetonitrile/0.1% TFA over 30 min and then continuously with 100% acetonitrile/0.1% TFA over 20 min at 1.0 cm^3 min^{-1} flow rate (R_t^1), and eluted with a linear gradient of 10–100% acetonitrile/0.1% TFA over 30 min at 1.0 cm^3 min^{-1} flow rate (R_t^2). Silica gel column chromatography was performed on Wakogel C-300 (Wako Pure Chemical Industries) in purifications. FAB-MS and MALDI TOF-MS spectroscopic measurements were performed on a JEOL JMS-SX 102A and Shimadzu Kratos Compact MALDI 3 mass spectrometers. Amino acid analyses were carried out on a JEOL JLC-300 system with ninhydrin detection after hydrolysis in 6.0 mol dm^{-3} HCl at 110 °C for 24 h in a sealed tube.

Preparations

Flavoenzyme models. Four different 53-Peptides were synthesized in the same manner as described by Mihara *et al.*[11,29] 7α-Bromoacetyl-10-methylisoalloxazine (Br-AcFl) was synthesized in the same manner as described by Levine and Kaiser.[30a]

Boc-D-Ala-Pro-Glu(OcHex)-Leu-Leu-Lys(ClZ)-OH (5), Boc-Cys(MeBzl)-Leu-Ala-Glu(OcHex)-Leu-Leu-Lys(ClZ)-OPip (-OPip = piperidyl ester, 6), Boc-Ala-Cys(MeBzl)-Ala-Glu(OcHex)-Leu-Leu-Lys(ClZ)-OPip (7), Boc-Ala-Leu-Cys-(MeBzl)-Glu(OcHex)-Leu-Leu-Lys(ClZ)-OPip (8), Boc-Ala-Leu-Ala-Glu(OcHex)-Leu-Leu-Lys(ClZ)-OPip (9), Boc-Ala-Leu-Ala-Glu(OcHex)-Leu-Leu-Lys(ClZ)-Gly-OBzl (10). Compounds **5**–**10** were prepared manually by stepwise elongation on *p*-nitrobenzophenone oxime resin[46] using benzotriazol-1-yloxytris(dimethylamino)phosphonium hexafluorophosphate (BOP)[47] and 1-hydroxybenzotriazole monohydrate (HOBt·H_2O) as described in our previous works. The obtained peptides were identified by FAB-MS: **5**, *m/z* 1043 [(M + Na)$^+$]; **6**, *m/z* 1327 [(M + H)$^+$]; **7**, *m/z* 1285 [(M + H)$^+$]; **8**, *m/z* 1327 [(M + H)$^+$]; **9**, *m/z* 1191 [(M + H)$^+$]; **10**, *m/z* 1255 [(M + H)$^+$].

Boc-(40–53)-OBzl (11). Compound **5** (1.74 g, 1.7 mmol) and H-Ala-Leu-Ala-Glu(OcHex)-Leu-Leu-Lys(ClZ)-Gly-OBzl·TFA obtained from **10** (2.13 g, 1.7 mmol) were condensed with 1-(3-dimethylaminopropyl)-3-ethylcarbodiimide hydrochloride (EDC·HCl) (489 mg, 2.55 mmol) in the presence of HOBt·H_2O (312 mg, 2.04 mmol) and triethylamine (0.24 cm^3, 1.7 mmol) in DMF at 0 °C for 24 h. The reaction mixture was concentrated and precipitated with water, and then washed with 4% $NaHCO_3$, 10% citric acid and water. The crude peptide was purified by reprecipitation with methanol–diethyl ether to yield **11** (3.06 g, 83%): HPLC R_t^1 = 39.00 min; FAB-MS *m/z* 2158 [(M + H)$^+$].

Boc-(1–13)-OH and Boc-(14–26)–OH (12). Compound **5** (1.74 g, 1.7 mmol) and H-Ala-Leu-Ala-Glu(OcHex)-Leu-Leu-Lys(ClZ)-OPip·TFA obtained from **9** (2.02 g, 1.7 mmol) were condensed in the same manner as for **11**. The reaction mixture was concentrated and precipitated with water, and then piperidyl ester was removed with sodium dithionite (5 equiv.) in acetic acid for 2 h at room temperature.[29b] The reaction mixture was concentrated and precipitated with water and the crude peptide purified by reprecipitation with methanol–diethyl ether to yield **12** (2.61 g, 63%). HPLC R_t^1 = 36.06 min; FAB-MS *m/z* 2033 [(M + Na)$^+$].

Boc-[Cys(MeBzl)^{33}]-(27–39)-OH (13). Compound **5** (296 mg, 0.29 mmol) and H-Cys(MeBzl)-Leu-Ala-Glu(OcHex)-Leu-Leu-Lys(ClZ)-OPip·TFA obtained from **6** (357 mg, 0.32 mmol) were condensed in the same manner as for **12**. The crude peptide was purified by reprecipitation with methanol–diethyl ether to yield **13** (443 mg, 73%). HPLC R_t^1 = 35.89 min; FAB-MS *m/z* 2170 [(M + Na)$^+$].

Boc-[Cys(MeBzl)^{34}]-(27–39)-OH (14). Compound **5** (1.77 g, 1.75 mmol) and H-Ala-Cys(MeBzl)-Ala-Glu(OcHex)-Leu-Leu-Lys(ClZ)-OPip·TFA obtained from **7** (2.25 g, 1.75 mmol) were condensed in the same manner as for **12**. The crude peptide was purified by reprecipitation with methanol–diethyl ether to yield **14** (2.61 g, 72%). HPLC R_t^1 = 33.98 min; FAB-MS *m/z* 2127 [(M + Na)$^+$].

Boc-[Cys(MeBzl)^{35}]-(27–39)-OH (15). Compound **5** (357 mg, 0.35 mmol) and H-Ala-Leu-Cys(MeBzl)-Glu(OcHex)-Leu-Leu-Lys(ClZ)-OPip·TFA obtained from **8** (430 mg, 0.39 mmol) were condensed in the same manner as for **12**. The crude peptide was purified by reprecipitation with methanol–diethyl ether to yield **15** (540 mg, 73%). HPLC R_t^1 = 36.34 min; FAB-MS *m/z* 2170 [(M + Na)$^+$].

Boc-[X_2^{33},X_3^{34},X_4^{35}]-(27–53)-OBzl (16a–c). Each of compounds **13**, **14**, and **15** (1.0 equiv.) and H-(40–53)-OBzl·TFA obtained from **11** was condensed in the same manner as for **11**. The crude peptide was purified by gel filtration chromatography on Sephadex LH-60 (DMF, 2.0 × 90 cm) to yield **16a** (X_2 = Cys(MeBzl)) (727 mg, 84%); **16b** (X_3 = Cys(MeBzl)) (1.14 g, 92%); **16c** (X_4 = Cys(MeBzl)) (801 mg, 89%).

Boc-[X_2^{33},X_3^{34},X_4^{35}]-(14–53)-OBzl (17a–c). Compound **12** (1.2 equiv.) and H-[X_2^{33},X_3^{34},X_4^{35}]-(27–53)-OBzl·TFA obtained from each of **16a**–**c** were condensed in the same manner as for **11**. The crude peptide was purified by gel filtration chromatography on Sephadex LH-60 (DMF, 2.0 × 90 cm) to yield **17a** (X_2 = Cys(MeBzl)) (743 mg, 68%); **17b** (X_3 = Cys(MeBzl)) (1.43 g, 53%); **17c** (X_4 = Cys(MeBzl)) (647 mg, 60%).

Boc-[X_1^8,X_2^{33},X_3^{34},X_4^{35}]-(1–53)-OBzl (18a–d). Compound **12** or **14** (1.2 equiv.) and H-[X_2^{33},X_3^{34},X_4^{35}]-(14–53)-OBzl·TFA

obtained from **17a**–**c** were condensed in the same manner as for **11**. The crude peptide was purified by gel filtration chromatography on Sephadex LH-60 (DMF, 2.0 × 90 cm) to yield **18a** (X_2 = Cys(MeBzl)) (477 mg, 69%); **18b** (X_3 = Cys(MeBzl)) (333 mg, 47%); **18c** (X_4 = Cys(MeBzl)) (457 mg, 69%); **18d** (X_1 and X_3 = Cys(MeBzl)) (587 mg, 41%).

H-[X_1^8,X_2^{33},X_3^{34},X_4^{35}]-(1–53)-OH (19a–d). Compounds **18a** (200 mg, 0.025 mmol), **18b** (292 mg, 0.037 mmol), **18c** (200 mg, 0.025 mmol) and **18d** (467 mg, 0.059 mmol) were treated with anhydrous HF (10 cm^3) in the presence of anisole (0.5 cm^3) and ethanedithiol (0.3 cm^3) at 0 °C for 90 min. After removal of HF, the peptides were extracted with 10% acetic acid and washed with diethyl ether. The aqueous layers were lyophilized to yield **19a** (X_2 = Cys) (156 mg (quant.), **19b** (X_3 = Cys) (192 mg, 92%), **19c** (X_4 = Cys) (150 mg (quant.)), and **19d** (X_1 and X_3 = Cys) (237 mg, 72%).

Flavin attachment. To each solution of compounds **19a**–**d** (50 mg, 9 μmol) of in 0.1 mol dm^{-3} Tris–HCl buffer, pH 7.5 (1.0 cm^3) was added Br-AcFl (10 mg, 27 μmol per cysteine residue) in dimethyl sulfoxide (1.0 cm^3). The resultant solution was stirred at room temperature for 5 h under a nitrogen atmosphere, then applied to a Sephadex G-50 gel filtration column (2.0 × 60 cm) preequilibrated with 10% acetic acid aqueous solution and then to a different size of Sephadex G-50 column (2.0 × 90 cm). These columns were eluted using 10% acetic acid aqueous solution and fractions of 2.0 cm^3 were collected. The flavin-bound 53-peptide was detected by its absorption at 430 nm. Then the collected fractions were evaporated and lyophilized. The final purification was carried out by HPLC equipped with a Superdex Peptide HR 10/30 (1.0 × 30 cm) GPC column eluted by 20% acetonitrile–0.1% TFA at 0.5 cm^3 min^{-1} flow rate. Finally, the collected fractions were lyophilized to give yellow powders: **1**, 33 mg (63%); **2**, 35 mg (67%); **3**, 34 mg (65%); **4**, 44 mg (80%). GPC analysis: **1**, 21.91 min; **2**, 21.99 min; **3**, 21.92 min; **4**, 21.73 min. Amino acid analysis: **1**, $Glu_{8.10}$(8), $Gly_{1.0}$(1), $Pro_{3.89}$(4), $Ala_{11.1}$(11), $Leu_{20.3}$(20), $Lys_{7.70}$(8); **2**, $Glu_{8.08}$(8), $Gly_{1.0}$(1), $Pro_{4.10}$(4), $Ala_{11.6}$(12), $Leu_{18.8}$(19), $Lys_{7.89}$(8); **3**, $Glu_{8.05}$(8), $Gly_{1.0}$(1), $Pro_{4.03}$(4), $Ala_{11.7}$(12), $Leu_{19.2}$(19), $Lys_{7.85}$(8); **4**, $Glu_{7.91}$(8), $Gly_{1.0}$(1), $Pro_{4.05}$(4), $Ala_{12.3}$(12), $Leu_{18.1}$(18), $Lys_{7.79}$(8).

1-Benzyl-1,4-dihydronicotinamide (benzyl-NAH). 1-Benzyl-1,4-dihydronicotinamide was synthesized as described by Mauzerall and Westheimer.[42] Its identity was confirmed by UV and MS spectroscopic analyses.

1-*n*-Butyl-1,4-dihydronicotinamide (*n*-butyl-NAH). *n*-Butyl iodide (4.05 g, 22.0 mmol) was added to a suspension of nicotinamide (1.2 g, 10 mmol) in acetonitrile (20 cm^3). The mixture was refluxed at 90 °C for 16 h and stood at room temperature. The crystals were filtered off and washed with acetonitrile and diethyl ether to yield the oxidized form (2.85 g, 92% yield). TLC (chloroform–methanol 5:1) R_f = 0.35; HPLC R_t^2 = 4.20 min; FAB-MS *m*/*z* 179 (M^+). Calc. ($C_{10}H_{15}N_2OI$): C, 39.23; H, 4.94; N, 9.15. Found: C, 39.21; H, 4.95; N, 9.20%.

1-Butylnicotinamide iodide was reduced in the same manner as described by Mauzerall and Westheimer.[42] 1-*n*-Butyl-1,4-dihydronicotinamide was prepared by adding 1-butylnicotinamide iodide (50 mg, 0.16 mmol) to a solution of anhydrous sodium carbonate (100 mg, 0.94 mmol) and sodium dithionite (200 mg, 1.15 mmol) in water (5.0 cm^3) at 50 °C. The reaction mixture was shaken for ten minutes. The solution was added to water (10 cm^3) and extracted with butan-1-ol–ethyl acetate (1:1 = v/v, 15 cm^3), but ethyl acetate (15 cm^3) for preparations of *n*-hexyl-, *n*-octyl-, *n*-decyl-, and *n*-dodecyl-NAHs. The organic phase was washed with water (10 cm^3 × 2) and concentrated by rotary evaporation. The crude product was purified by silica gel column chromatography eluted with 9:1 chloroform–methanol. The yellow oily product was diluted with methanol and used in assays. The identity of *n*-butyl-NAH was confirmed by λ_{max} at 360 nm. TLC (chloroform–methanol 9:1) R_f 0.39.

1-*n*-Hexyl-1,4-dihydronicotinamide (*n*-hexyl-NAH). 1-Hexylnicotinamide iodide was synthesized from nicotinamide and *n*-hexyl iodide in the same manner as *n*-butyl-NAH. Yield 2.59 g (78%). TLC (chloroform–methanol 5:1) R_f 0.35; HPLC R_t^2 = 12.03 min; FAB-MS *m*/*z* 207 (M^+). Calc. ($C_{12}H_{19}N_2OI$): C, 43.13; H, 5.73; N, 8.38. Found: C, 43.42; H, 5.70; N, 8.39%.

1-Hexylnicotinamide iodide was reduced to obtain *n*-hexyl-NAH. TLC (chloroform–methanol 9:1) R_f 0.63.

1-*n*-Octyl-1,4-dihydronicotinamide (*n*-octyl-NAH). 1-Octylnicotinamide iodide was synthesized from nicotinamide and *n*-octyl iodide in the same manner as *n*-butyl-NAH. Yield 2.54 g (78%). TLC (chloroform–methanol 5:1) R_f 0.48. HPLC R_t^2 = 16.23 min; FAB-MS *m*/*z* 235 (M^+). Calc. ($C_{14}H_{23}N_2OI$): C, 46.42; H, 6.40; N, 7.73. Found: C, 46.41; H, 6.34; N, 7.68%.

1-Octylnicotinamide iodide was reduced to obtain *n*-octyl-NAH. TLC (chloroform–methanol 9:1) R_f 0.70.

1-*n*-Decyl-1,4-dihydronicotinamide (*n*-decyl-NAH). 1-Decylnicotinamide iodide was synthesized from nicotinamide and *n*-decyl iodide in the same manner as *n*-butyl-NAH. Yield 2.36 g (61%). TLC (chloroform–methanol 5:1) R_f 0.41; HPLC R_t^2 = 19.27 min; FAB-MS *m*/*z* 263 (M^+). Calc. ($C_{16}H_{27}N_2OI$): C, 49.24; H, 6.97; N, 7.18. Found: C, 49.18; H, 6.87; N, 7.11%.

1-Decylnicotinamide iodide was reduced to obtain *n*-decyl-NAH. TLC (chloroform–methanol 9:1) R_f 0.68.

1-*n*-Dodecyl-1,4-dihydronicotinamide (*n*-dodecyl-NAH). 1-Dodecylnicotinamide iodide was synthesized from nicotinamide and *n*-dodecyl iodide in the same manner as *n*-butyl-NAH. Yield 1.17 g (28%). TLC (chloroform–methanol 5:1) R_f 0.16; HPLC R_t^2 = 21.71 min; FAB-MS *m*/*z* 291 (M^+). Calc. ($C_{18}H_{31}N_2OI$): C, 51.68; H, 7.47; N, 6.70. Found: C, 51.60; H, 7.49; N, 6.74%.

1-Dodecylnicotinamide iodide was reduced to obtain *n*-dodecyl-NAH. TLC (chloroform–methanol 9:1) R_f 0.47.

Solution molecular mass determination

Gel filtration chromatography was performed on a Hitachi HPLC system equipped with a Hitachi L-6300 Intelligent Pump, L-4200 UV-VIS Detector and D-2500 Chromato Integrator. A Superdex Peptide HR 10/30 (1.0 × 30 cm, Pharmacia Biotech) was used and eluted with 20% acetonitrile–0.1% TFA in water, flow rate 0.5 cm^3 min^{-1} at 25 °C. A 3.0×10^{-5} mol dm^{-3} sample peptide solution in 0.1 M Tris–HCl buffer, pH 7.5 containing 1% methanol was prepared. A 0.025 cm^3 volume of this solution was loaded for HPLC. The column was calibrated by cytochrome *c* (molecular weight 12400), aprotinin (bovine lung, 6500) and insulin B-chain (bovine, 3496).

UV/vis spectroscopy

UV/vis spectra were recorded on a Hitachi U-3000 spectrophotometer. The **1**, **2**, and **3** peptide concentrations were determined by using ε_{430} = 11000 dm^3 mol^{-1} cm^{-1}, and the **4** peptide concentration by using ε_{430} = 21800 dm^3 mol^{-1} cm^{-1} for two oxidized flavin derivatives.[30a] The concentration of substrate was determined by using ε_{360} = 7300 dm^3 mol^{-1} cm^{-1} in 0.1 mol dm^{-3} Tris–HCl buffer, pH 7.5.

CD spectropolarimetry

CD spectra were acquired on a JASCO J-500A spectropolarimeter, routinely calibrated with (+)-camphor-10-sulfonic acid. The samples were prepared in 0.1 mol dm^{-3} Tris–HCl buffer, pH 7.5 with various methanol contents and typical spectra were measured using 1.0 mm cuvettes in the wavelength interval

250 to 200 nm. We calculated α-helicity using the following equation: $[\theta]_{max}(100\%\ \alpha\text{-helix}) = [\theta][(n-4)/n]$, where $[\theta]$ is -40000 deg cm^2 dmol^{-1} according to Lyu *et al.*[38] When $n = 53$, $[\theta]_{max}(100\%\ \alpha\text{-helix}) = -37000$ deg cm^2 dmol^{-1} was obtained.

Fluorescence spectroscopy

Fluorescence spectra were acquired on a Hitachi F-2500 fluorescence spectrophotometer at 25 °C in 0.1 mol dm^{-3} Tris–HCl buffer, pH 7.5 with various methanol contents. Spectra excited at 430 nm were measured using 1.0 cm cuvettes in the wavelength interval 440 to 630 nm. Fluorescence quenching parameters were determined from the Stern–Volmer equation: $F_0/F = (1 + K_{SV}[Q])\exp([Q]v)$, where F_0 and F are the flavin fluorescence intensities in the absence and presence of quencher, respectively, K_{SV} is the Stern–Volmer quenching constant, [Q] the sodium iodide (quencher) concentration, and V the volume of the quenching sphere.[34,40]

Kinetic measurements

The 53-peptides were dissolved in methanol to give stock solutions, and substrates were also so dissolved. A 0.1 mol dm^{-3} Tris–HCl buffer was transferred to a 1.0 cm quartz cuvette followed by substrate and peptide stock solutions, respectively. The final conditions were as follows: 0.1 mol dm^{-3} Tris–HCl buffer containing 2% methanol for benzyl-NAH with the series of sodium *n*-alkanesulfonates and 12% methanol for the series of 1-*n*-alkyl-1,4-dihydronicotinamides, pH 7.5 at 25 °C. The cuvette was shaken and immediately placed in the UV/vis spectrometer (Hitachi U-3000 spectrophotometer) to measure the absorbance at 360 nm. The decrease in absorbance according to the consumption of alkyl-NAHs was monitored for 15 min to collect the initial rates (v_0). The apparent kinetic parameters (k_{cat}, K_M, and k_{cat}/K_M) were given by the curve fitting (KaleidaGraph, Synergy Software) with the Michaelis–Menten equation, $v_0 = k_{cat}[peptide][S]/(K_M + [S])$, of substrate concentration *vs.* v_0 plots, where [peptide] is the total peptide concentration and [S] the substrate concentration.

Acknowledgements

This work was partly supported by Grants-in-Aid (No. 08878087 and No. 10480153 to N. N.) from the Ministry of Education, Science and Culture, Japan.

References

1 S. P. Ho and W. F. DeGrado, *J. Am. Chem. Soc*, 1987, **109**, 6751.
2 S. F. Betz, D. P. Raleigh and W. F. DeGrado, *Curr. Opin. Struct. Biol.*, 1993, **3**, 601.
3 S. F. Betz, J. W. Bryson and W. F. DeGrado, *Curr. Opin. Struct. Biol.*, 1995, **5**, 457.
4 J. W. Bryson, S. F. Betz, H. S. Lu, D. J. Suich, H. X. Zhou, K. T. O'Neil and W. F. DeGrado, *Science*, 1995, **270**, 935.
5 (*a*) M. Mutter and S. Vuilleumier, *Angew. Chem., Int. Ed. Engl.*, 1989, **28**, 535; (*b*) G. Tuchscherer, L. Scheibler, P. Dumy and M. Mutter, *Biopolymers*, 1998, **47**, 63.
6 P. E. Dawson and S. B. H. Kent, *J. Am. Chem. Soc.*, 1993, **115**, 7263.
7 D. P. Raleigh and W. F. DeGrado, *J. Am. Chem. Soc.*, 1992, **114**, 10079.
8 T. M. Handel, S. A. Williams and W. F. DeGrado, *Science*, 1993, **261**, 879.
9 T. M. Handel, S. A. Williams, D. Menyhard and W. F. DeGrado, *J. Am. Chem. Soc.*, 1993, **115**, 4457.
10 N. Nishino, H. Mihara, T. Uchida and T. Fujimoto, *Chem. Lett.*, 1993, 53.
11 (*a*) N. Nishino, H. Mihara, Y. Tanaka and T. Fujimoto, *Tetrahedron Lett.*, 1992, **33**, 5767; (*b*) H. Mihara, Y. Tanaka, T. Fujimoto and N. Nishino, *J. Chem. Soc., Perkin Trans. 2*, 1995, 1915; (*c*) Y. Tanaka, K. Nagamoto, H. Sasaki, T. Fujimoto, N. Nishino and M. Oka, *Tetrahedron Lett.*, 1996, **37**, 881.
12 J. Baum, C. M. Dobson, P. A. Evans and C. Hanley, *Biochemistry*, 1989, **28**, 7.
13 T. Sasaki and E. T. Kaiser, *J. Am. Chem. Soc.*, 1989, **111**, 380.
14 K. S. Åkerfeldt, R. M. Kim, D. Camac, J. T. Groves, J. D. Lear and W. F. DeGrado, *J. Am. Chem. Soc.*, 1992, **114**, 9656.
15 H. Mihara, K. Tomizaki, T. Fujimoto, S. Sakamoto, H. Aoyagi and N. Nishino, *Chem. Lett.*, 1996, 187.
16 (*a*) C. T. Choma, J. D. Lear, M. J. Nelson, P. L. Dutton, D. E. Robertson and W. F. DeGrado, *J. Am. Chem. Soc.*, 1994, **116**, 856; (*b*) D. E. Robertson, R. S. Farid, C. C. Moser, J. L. Urbauer, S. E. Mulholland, R. Pidikiti, J. D. Lear, A. J. Wand, W. F. DeGrado and P. L. Dutton, *Nature* (*London*), 1994, **368**, 425.
17 H. K. Rau and W. Haehnel, *J. Am. Chem. Soc.*, 1998, **120**, 468.
18 K. Johnsson, R. K. Allemann, H. Widmer and S. A. Benner, *Nature* (*London*), 1993, **365**, 530.
19 K. S. Broo, L. Brive, P. Ahlberg and L. Baltzer, *J. Am. Chem. Soc.*, 1997, **119**, 11362.
20 K. Broo, H. Nilsson, J. Nilsson, A. Flodberg and L. Baltzer, *J. Am. Chem. Soc.*, 1998, **120**, 4063.
21 K. S. Broo, H. Nilsson, J. Nilsson and L. Baltzer, *J. Am. Chem. Soc.*, 1998, **120**, 10287.
22 L. Andersson, G. Stenhagen and L. Baltzer, *J. Org. Chem.*, 1998, **63**, 1366.
23 M. Allert, M. Kjellstrand, K. S. Broo, Å. Nilsson and L. Baltzer, *Chem. Commun.*, 1998, 1547.
24 C. Walsh, *Acc. Chem. Res.*, 1980, **13**, 148.
25 T. C. Bruice, *Acc. Chem. Res.*, 1980, **13**, 256.
26 V. Massey and P. Hemmerich, in *The Enzymes*, 3rd edn, ed. P. D. Boyer, Academic Press, New York, 1975, vol. 12, Part B, p. 191.
27 D. P. Ballou, in *Flavins and Flavoproteins*, eds. V. Massey and C. H. Williams, Elsevier North Holland, Inc., Amsterdam, 1982, ch. 48, p. 301.
28 H. Mihara, K. Tomizaki, N. Nishino and T. Fujimoto, *Chem. Lett.*, 1993, 1533.
29 (*a*) E. T. Kaiser, H. Mihara, G. A. Laforet, J. W. Kelly, L. Walters, M. A. Findeis and T. Sasaki, *Science*, 1989, **243**, 187; (*b*) T. Sasaki, M. A. Findeis and E. T. Kaiser, *J. Org. Chem.*, 1991, **56**, 3159; (*c*) J. C. Hendrix, K. J. Halverson and P. T. Lansbury, Jr., *J. Am. Chem. Soc.*, 1992, **114**, 7930; (*d*) H. Mihara, J. A. Chmielewski and E. T. Kaiser, *J. Org. Chem.*, 1993, **58**, 2209.
30 (*a*) H. L. Levine and E. T. Kaiser, *J. Am. Chem. Soc.*, 1978, **100**, 7670; (*b*) J. P. Germanas and E. T. Kaiser, *Biopolymers*, 1990, **29**, 39.
31 D. Hilvert and E. T. Kaiser, *J. Am. Chem. Soc.*, 1985, **107**, 5805.
32 S. E. Rokita and E. T. Kaiser, *J. Am. Chem. Soc.*, 1986, **108**, 4984.
33 T. Kokubo, S. Sassa and E. T. Kaiser, *J. Am. Chem. Soc.*, 1987, **109**, 606.
34 R. E. Sharp, C. C. Moser, F. Rabanal and P. L. Dutton, *Proc. Natl. Acad. Sci. U.S.A.*, 1998, **95**, 10465.
35 M. B. Twitchet, J. C. Ferrer, P. Siddarth and A. G. Mauk, *J. Am. Chem. Soc.*, 1997, **119**, 435.
36 W. König and R. Geiger, *Chem. Ber.*, 1970, **103**, 788.
37 (*a*) H. Kuang, M. L. Brown, R. R. Davies, E. C. Young and M. D. Distefano, *J. Am. Chem. Soc.*, 1996, **118**, 10702; (*b*) R. R. Davies and M. D. Distefano, *J. Am. Chem. Soc.*, 1997, **119**, 11643.
38 P. C. Lyu, J. C. Sherman, A. Chen and N. R. Kallenbach, *Proc. Natl. Acad. Sci. U.S.A.*, 1991, **88**, 5317.
39 M. C. Falk and D. B. McCormick, *Biochemistry*, 1976, **15**, 646.
40 P. I. H. Bastiaens, A. van Hoek, W. J. H. van Berkel, A. de Kok and A. J. W. G. Visser, *Biochemistry*, 1992, **31**, 7061.
41 Y. Tanaka, H. Akisada, T. Fujimoto and N. Nishino, *Chem. Lett.*, 1996, 135.
42 D. Mauzerall and F. H. Westheimer, *J. Am. Chem. Soc.*, 1955, **77**, 2261.
43 F. Jabolonski and M. DeLuca, *Biochemistry*, 1977, **16**, 2932.
44 T. Honma and Y. Ogura, *Biochim. Biophys. Acta*, 1977, **484**, 9.
45 W. F. DeGrado, *Nature* (*London*), 1993, **365**, 488.
46 W. F. DeGrado and E. T. Kaiser, *J. Org. Chem.*, 1980, **45**, 1295.
47 B. Castro, J. R. Dormoy, G. Evin and C. Selve, *Tetrahedron Lett.*, 1975, 1219.

Paper a907730h